Electronic Supplementary Material (ESI) for Environmental Science: Nano.

Supporting Information

(24 pages)

Ultrathin $Bi_4O_5Br_2$ nanosheets with surface oxygen vacancies and strong interaction with $Bi_2O_2CO_3$ for highly efficient removal of water contaminants

Lili Zhang,[a] Zhiqiang Wang,[a] Tong Li,[b] Chun Hu*[ab] and Min Yang[a]

[a] Key Laboratory of Drinking Water Science and Technology, Research Center for Eco-Environmental Sciences, Chinese Academy of Sciences, Beijing, 100085, China

[b] Institute of Environmental Research at Greater Bay, Key Laboratory for Water Quality and Conservation of the Pearl River Delta, Ministry of Education, Guangzhou University, Guangzhou, 510006, China

Corresponding Author: Chun Hu

Tel: +86 10 62843038

Fax: +86 10 62923541

Email: huchun@rcees.ac.cn, huchun@gzhu.edu.cn.

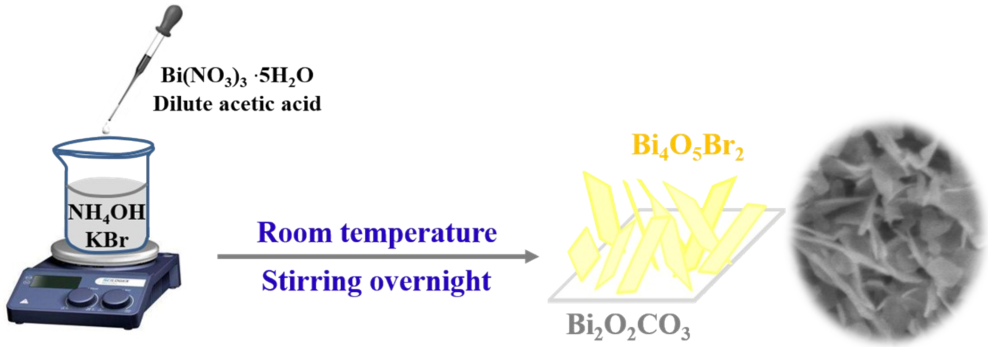

Scheme S1 Schematic illustration of the facile synthetic process of $Bi_4O_5Br_2/Bi_2O_2CO_3$.

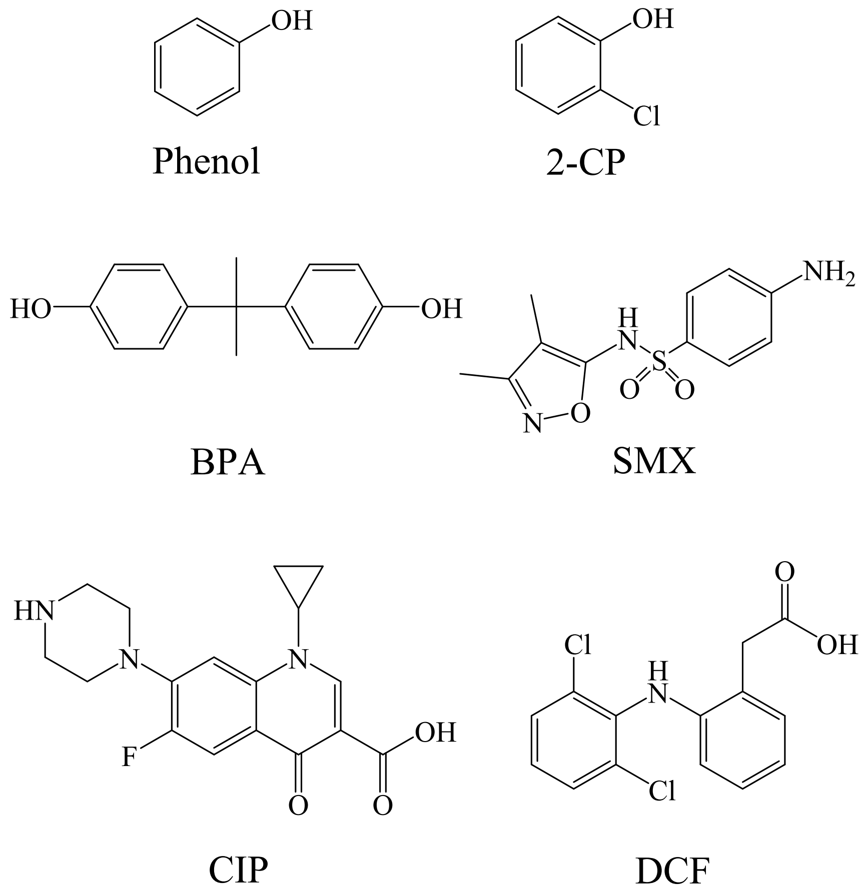

Scheme S2 Structures of phenol, 2-chlorophenol (2-CP), bisphenol A (BPA), sulfamethoxazole (SMX), ciprofloxacin (CIP) and diclofenac (DCF).

Table S1 Element composition of the $Bi_4O_5Br_2/Bi_2O_2CO_3$ samples.

Sample	Mass content of $Bi_4O_5Br_2$		Br/Bi molar ratio		
	Bulk (XRF)	Bulk (IC+ICPOES)	Surface (XPS)	Bulk (XRF)	Bulk (IC+ICPOES)
a	0 wt%	0 wt%	0	0	0
b	10.5 wt%	7.2 wt%	0.0424	0.0501	0.0341
c	18.4 wt%	13.3 wt%	0.0664	0.0879	0.0633
d	26.2 wt%	18.3 wt%	0.0949	0.1260	0.0878
e	36.4 wt%	34.3 wt%	0.1465	0.1756	0.1655
f	49.0 wt%	40.1 wt%	0.1946	0.2381	0.1941

Table S2 The catalytic performance comparison of previously reported photocatalysts for pollutants degradation.

Catalyst	Pollutant (mg L^{-1})	Removal efficiency	Mineralization efficiency	Operating conditions	Ref
$Bi_4O_5Br_2/Bi_2O_2CO_3$	2-CP (10)	100% (60 min)	85 % (60 min)	5W LED (400-800 nm)	This work
$Bi_4O_5Br_2/Bi_2O_2CO_3$	BPA (10)	100% (15 min)	62% (60 min)	5W LED (400-800 nm)	This work
$Pd/Bi_4O_5Br_2$ (1.0 wt% Pd)	BPA (20)	95.8% (70 min)	-	5W white LED light (400-800 nm)	[S1]
graphene/g-C_3N_4	2-CP (10)	85% (60 min)	-	LED light (400-800 nm)	[S2]
graphene/g-C_3N_4	BPA (10)	99% (60 min)	80% (60 min)	LED light (400-800 nm)	[S2]
Bi-$Bi_{2-\delta}MoO_6$-0.2	2-CP (10)	89% (180 min)	61.7% (180 min)	150W Xe lamp > 400 nm	[S3]
$I_{0.30}$-Bi_2WO_6	2-CP (10)	100% (240 min)	72.9% (300 min)	150W Xe lamp > 400 nm	[S4]
BiOI-110	BPA (10)	95% (300 min)	95% (300 min)	500 W Xe lamp	[S5]
BiOBr-OV	BPA	35%	-	300 W Xe	[S6]

	(10)	(150 min)	lamp

Table S3 The comparison for element ratio of the fresh and used $Bi_4O_5Br_2/Bi_2O_2CO_3$.

Atom ratio	XPS		EDS	
	Fresh	Used	Fresh	Used
C/Bi	0.7988	0.9092	1.4867	1.9983
O/Bi	1.5189	1.6421	1.2362	2.4112
Br/Bi	0.1465	0.1265	0.2405	0.2859

Table S4 The main products during the photocatalytic degradation of DCF in $Bi_4O_5Br_2/Bi_2O_2CO_3$ suspension at different reaction times, as detected by HPLC-QTOF-MS.

0 min

Retention time (min)	Molecular structure	Name	m/z
Main products on the surface of the catalyst			
9.22	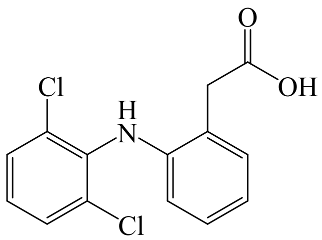	2-(2-((2,6-dichlorophenyl)amino)phenyl)acetic acid (DCF)	294
Main products in the aqueous solution			
9.14	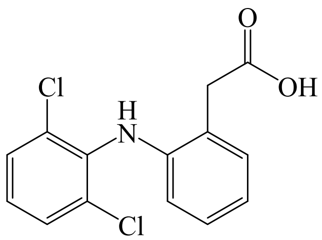	2-(2-((2,6-dichlorophenyl)amino)phenyl)acetic acid (DCF)	294

60 min

Retention time (min)	Molecular structure	Name	m/z
Main products on the surface of the catalyst			
9.17	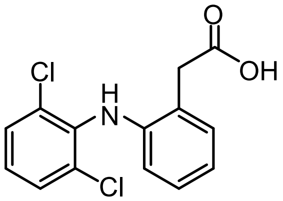	2-(2-((2,6-dichlorophenyl)amino)phenyl)acetic acid (DCF)	294
Main products in the aqueous solution			

7.70	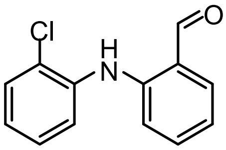	(2-((2-chlorophenyl)amino)phenyl) methyl aldehyde	228
8.10	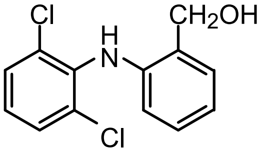	(2-((2,6-dichlorophenyl)amino)phenyl)methanol	266
9.16	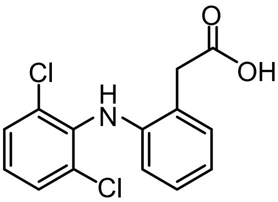	2-(2-((2,6-dichlorophenyl)amino)phenyl)acetic acid (DCF)	294

180 min

Retention time (min)	Molecular structure	Name	m/z
Main products on the surface of the catalyst			
9.17	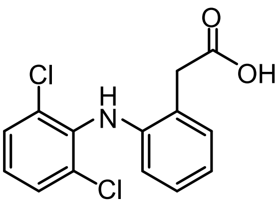	2-(2-((2,6-dichlorophenyl)amino)phenyl)acetic acid (DCF)	294
Main products in the aqueous solution			
3.51	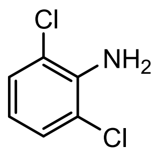	2,6-dichloroaniline	160
5.06	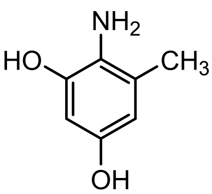	2,4-dihydroxy-6-methylaniline	138

6.06	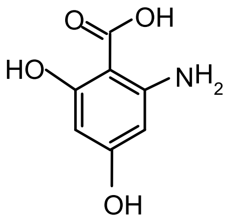	2,4-dihydroxy-6-aminobenzoic acid	168
7.64	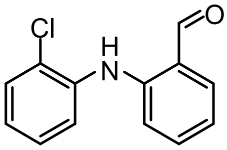	(2-((2-chlorophenyl)amino)phenyl) methyl aldehyde	228
8.10	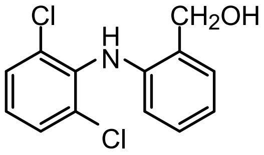	(2-((2,6-dichlorophenyl)amino)phenyl)methanol	266
9.15	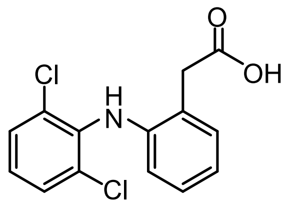	2-(2-((2,6-dichlorophenyl)amino)phenyl)acetic acid (DCF)	294

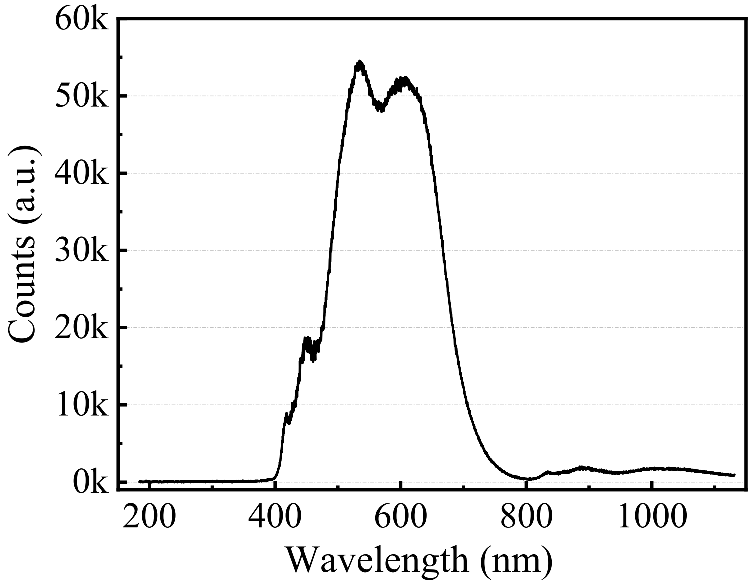

Fig. S1 Spectral distribution of the LED lamp bead used in this work.

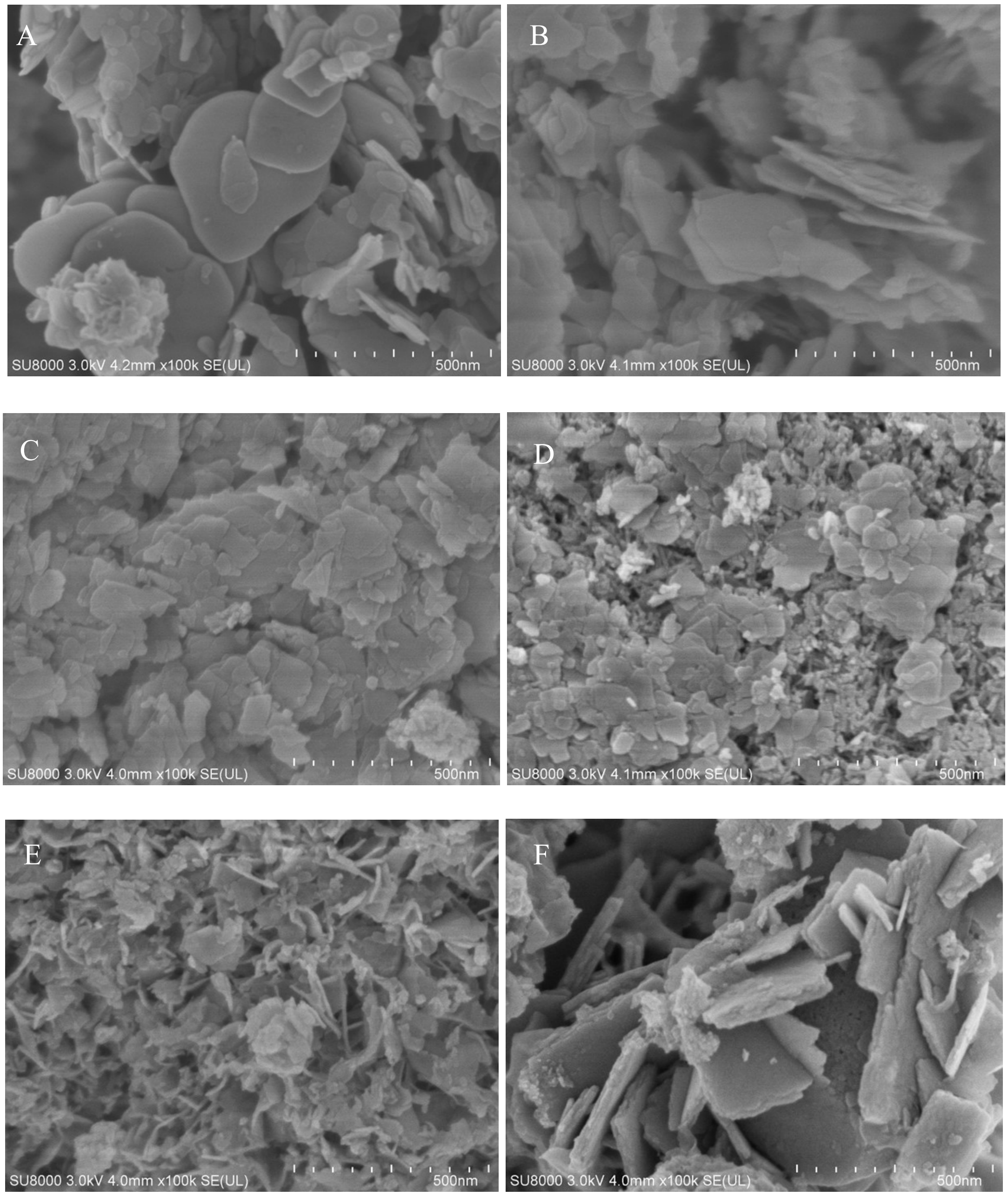

Fig. S2 SEM images of (A) $Bi_2O_2CO_3$, (B-E) 10.5, 18.4, 26.2, and 49.0 wt% $Bi_4O_5Br_2/Bi_2O_2CO_3$, (F) $Bi_4O_5Br_2$.

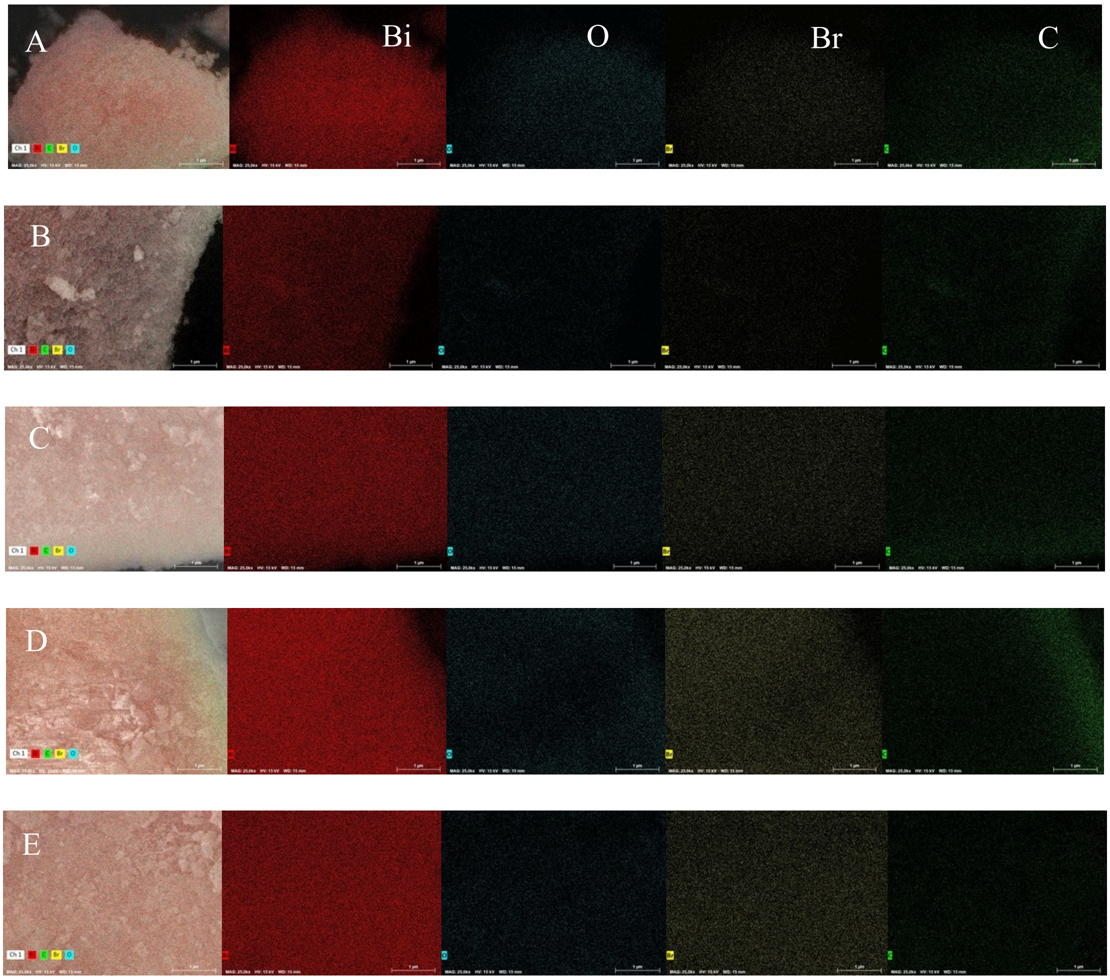

Fig. S3 SEM elemental mapping results of (A-E) 10.5-49.0 wt% $Bi_4O_5Br_2/Bi_2O_2CO_3$.

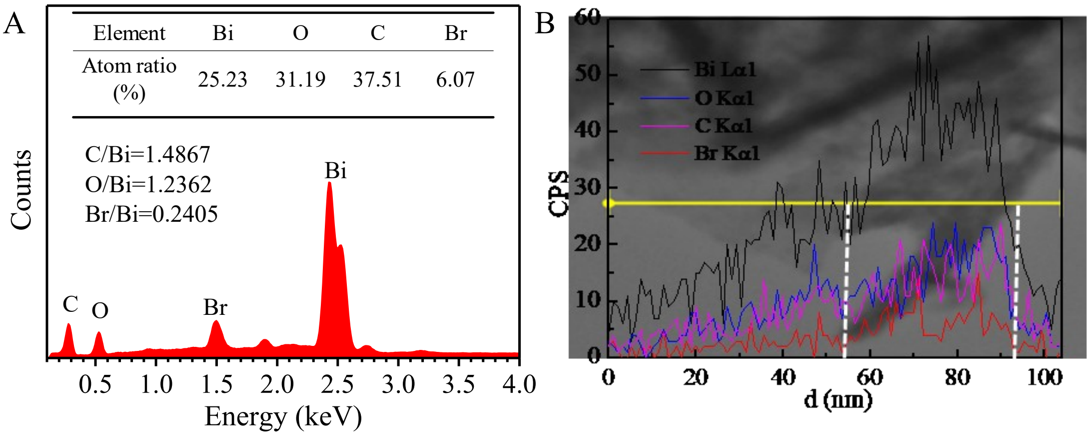

Fig. S4 (A) SEM EDS spectrum, and (B) TEM line scan spectra of $Bi_4O_5Br_2/Bi_2O_2CO_3$.

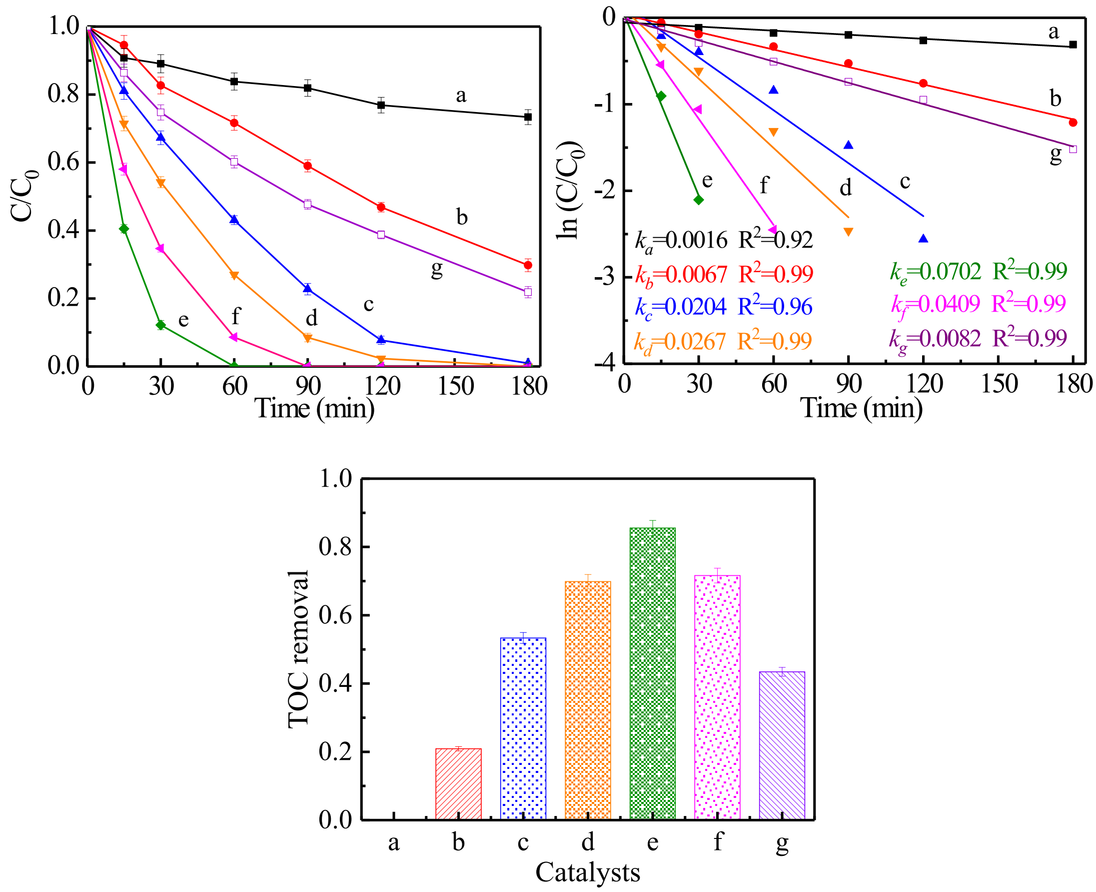

Fig. S5 2-CP degradation, kinetics, and TOC removal in different suspensions: (a) $Bi_2O_2CO_3$, (b-f) 10.5-49.0 wt% $Bi_4O_5Br_2/Bi_2O_2CO_3$, (g) $Bi_4O_5Br_2$. Experimental condition: $[2\text{-CP}]_0$=10 mg L^{-1}, catalyst dosage=1.6 g L^{-1}, light source: visible LED.

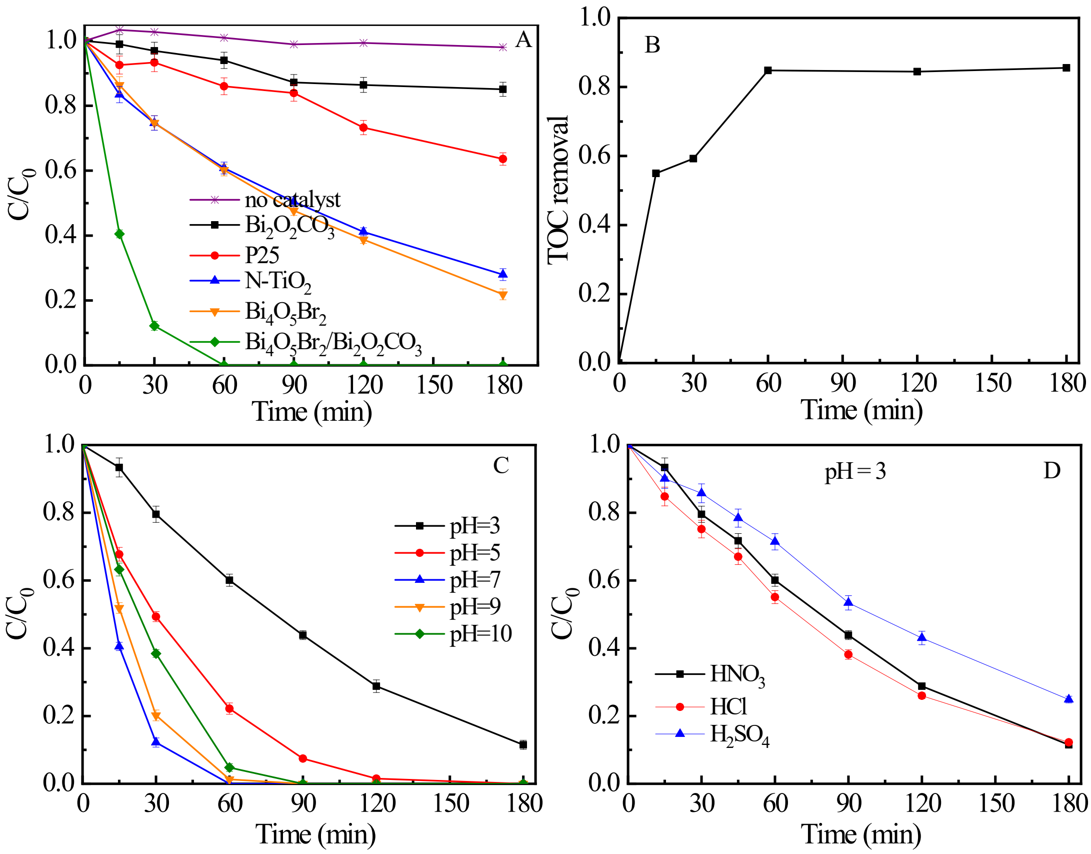

Fig. S6 (A) The comparison of 2-CP degradation for different catalysts, (B) TOC removal curve over time, (C) Effect of pH on degradation of 2-CP by $Bi_4O_5Br_2/Bi_2O_2CO_3$, and (D) Effect of the pH regulating solutes. Experimental condition: $[2\text{-CP}]_0$=10 mg L^{-1}, catalyst dosage=1.6 g L^{-1}, light source: visible LED.

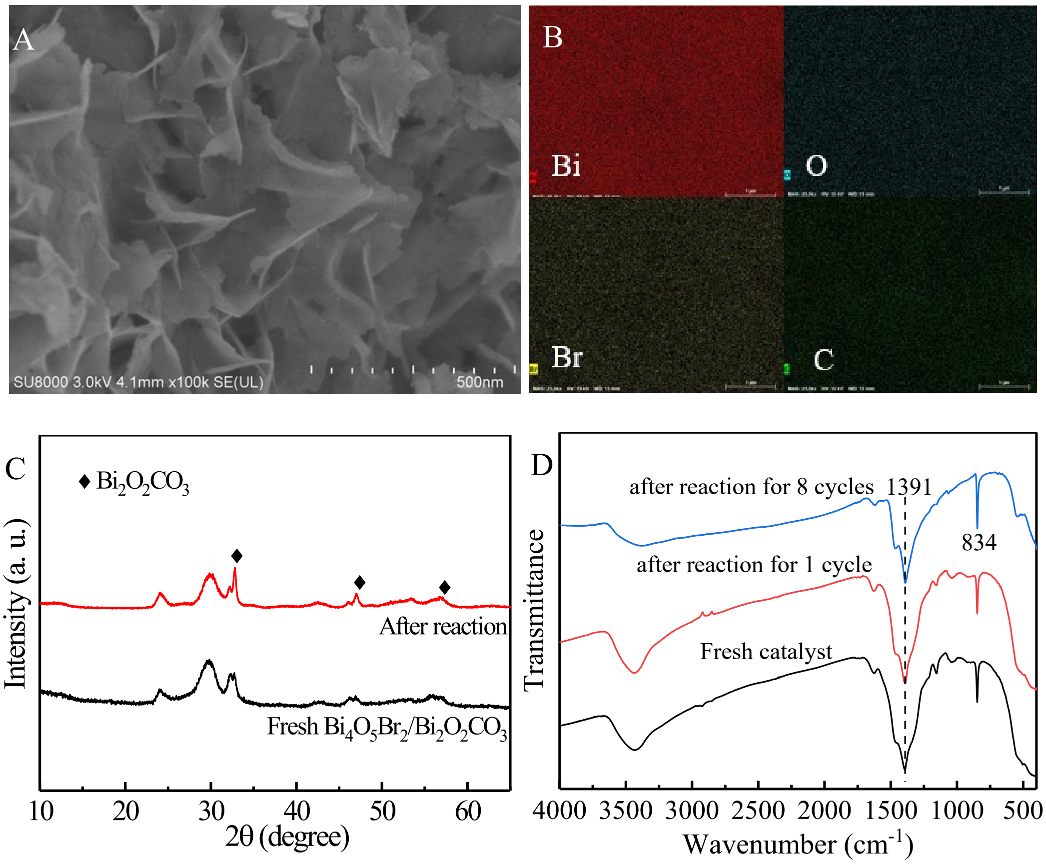

Fig. S7 SEM image, elemental mapping, XRD and FTIR spectra of $Bi_4O_5Br_2/Bi_2O_2CO_3$ after reaction.

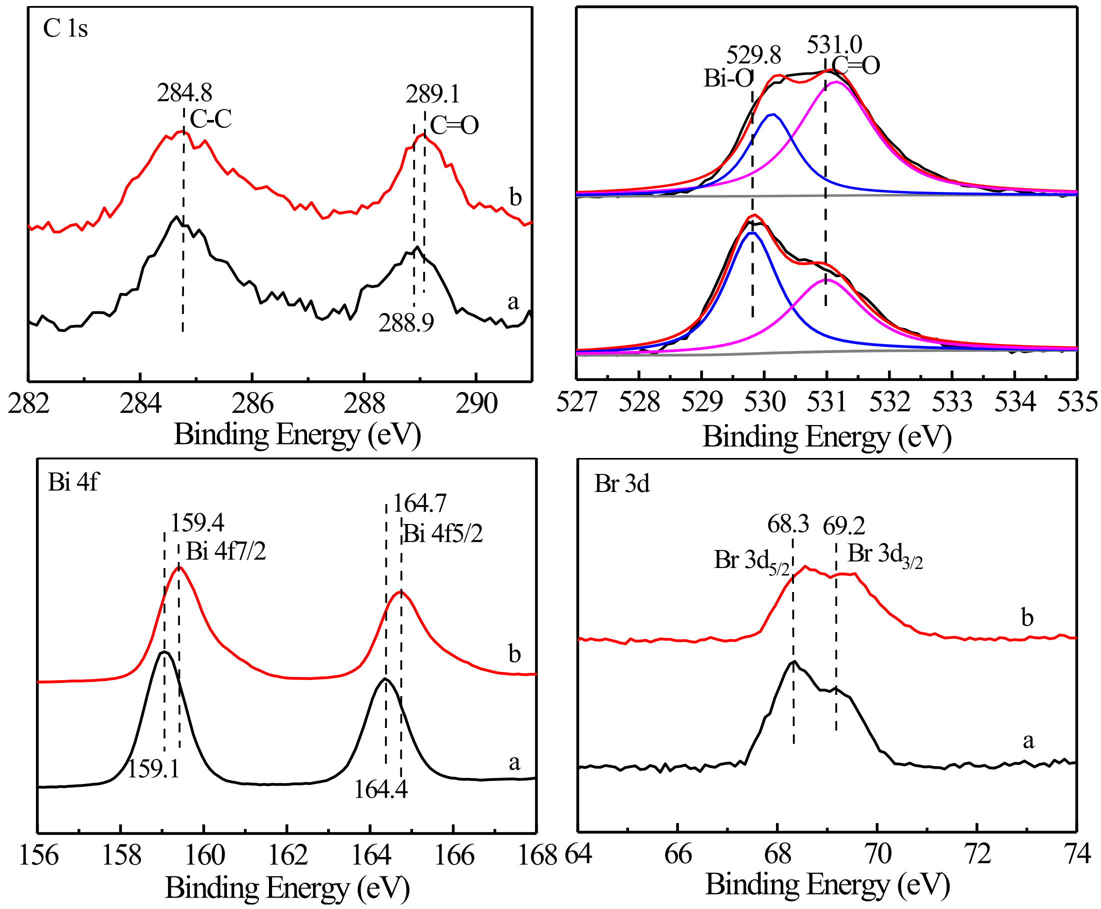

Fig. S8 The high-resolution C 1s, O 1s, Bi 4f and Br 3d XPS spectra of $Bi_4O_5Br_2/Bi_2O_2CO_3$: (a) before and (b) after reaction.

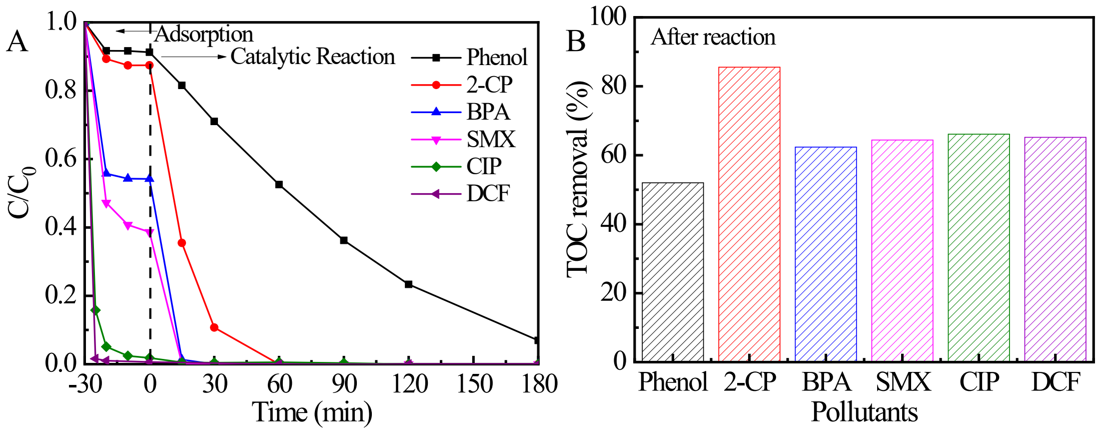

Fig. S9 (A) Adsorption and degradation of different pollutants; (B) The corresponding TOC removal in $Bi_4O_5Br_2/Bi_2O_2CO_3$ suspension. Experimental condition: $[Pollutant]_0$=10 mg L^{-1} or $[DCF]_0$=24.8 mg L^{-1}, catalyst dosage=1.6 g L^{-1}, light source: visible LED.

Degradation process of various pollutants

$Bi_4O_5Br_2/Bi_2O_2CO_3$ showed satisfactory treatment performance for various pollutants, such as phenol, bisphenol A (BPA), sulfamethoxazole (SMX), ciprofloxacin (CIP) and diclofenac (DCF). The removal process of these typical pollutants over $Bi_4O_5Br_2/Bi_2O_2CO_3$ under visible LED was investigated. As illustrated in Fig. S9, around 10% of adsorption for phenol and 2-CP (both with a hydroxyl group), 46% of adsorption for BPA (with two hydroxyl groups), 60% of adsorption for SMX (with a sulfanilamide group), and nearly complete adsorption for CIP and DCF (both with a carboxylic acid group) were observed. The results indicated that the functional groups of pollutants are key for their adsorption on $Bi_4O_5Br_2/Bi_2O_2CO_3$. Accordingly, complete removal of phenol substrate from water needed more than 180 min reaction, while only 60 min or about 15 min was required for 2-CP or BPA and SMX. For CIP and DCF, no desorption was observed during 180 min reaction under visible LED. The solution TOC removal reached over 60% for nearly all the tested pollutants.

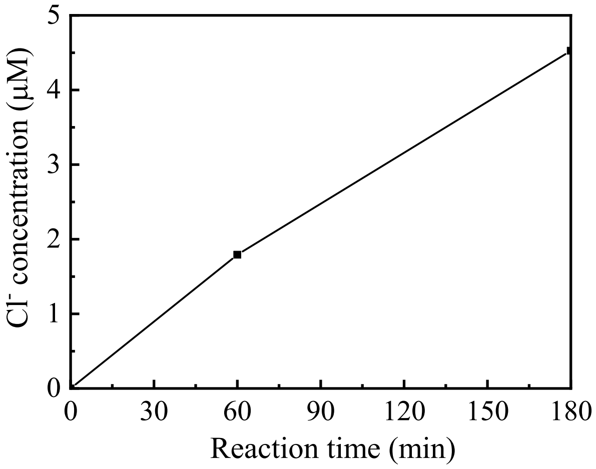

Fig. S10 The generation of Cl^- during DCF degradation.

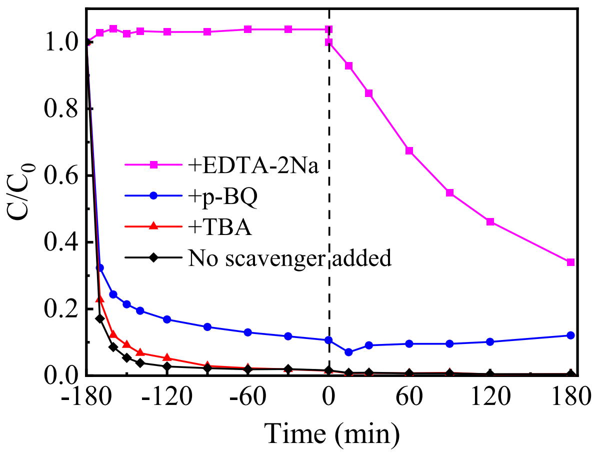

Fig. S11 Effect of reactive species scavengers on DCF degradation in $Bi_4O_5Br_2/Bi_2O_2CO_3$ suspension under visible LED.

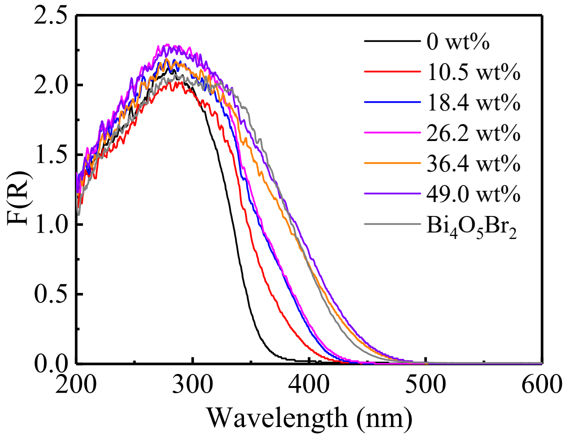

Fig. S12 Spectral absorbance of $Bi_4O_5Br_2/Bi_2O_2CO_3$ with various $Bi_4O_5Br_2$ weight percentages.

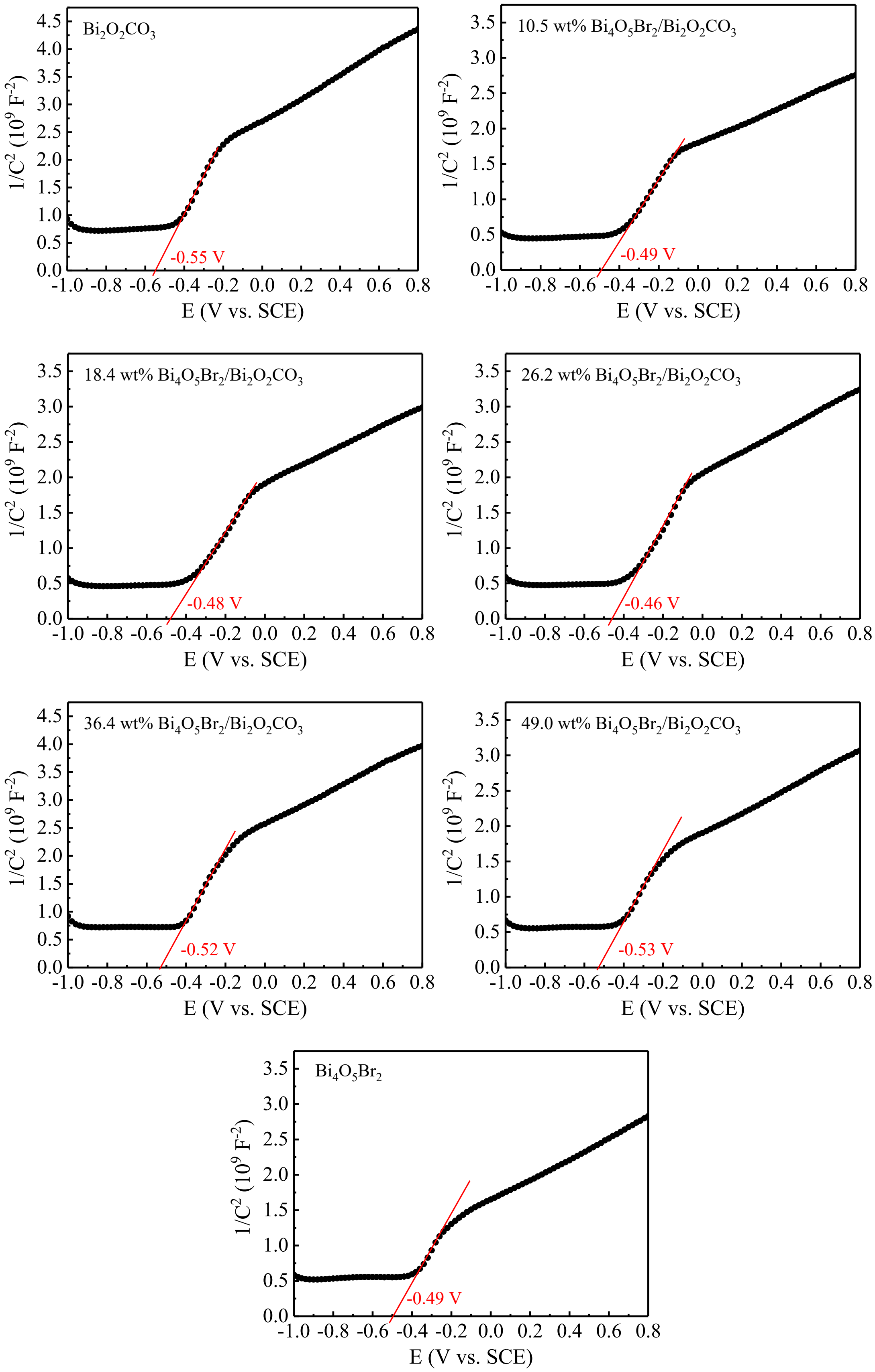

Fig. S13 The Mott-Schottky plots of $Bi_4O_5Br_2/Bi_2O_2CO_3$ with various $Bi_4O_5Br_2$ weight percentages in 0.1 M Na_2SO_4 aqueous solution (pH 6.60).

References

S1 N. Li, G. Zhu, M. Hojamberdiev, R. Zhu, J. Chang, J. Gao, Q. Guo, P. Liu, Pd nanoparticle-decorated $Bi_4O_5Br_2$ nanosheets with enhanced visible-light photocatalytic activity for degradation of bisphenol A, J. Photochem. Photobio. A: Chem. 356, (2018) 440–450.

S2 F. Li, M. Tang, T. Li, L. Zhang, C. Hu, Two-dimensional graphene/g-C_3N_4 in-plane hybrid heterostructure for enhanced photocatalytic activity with surface-adsorbed pollutants assistant, Appl. Catal. B: Environ. 268 (2020) 118397.

S3 L. Zhang, Z. Wang, C. Hu, B. Shi, Enhanced photocatalytic performance by the synergy of Bi vacancies and Bi^0 in Bi^0-$Bi_{2-\delta}MoO_6$, Appl. Catal. B: Environ. 257 (2019) 117785.

S4 L. Wang, Z. Wang, L. Zhang, C. Hu, Enhanced photoactivity of Bi_2WO_6 by iodide insertion into the interlayer for water purification under visible Light, Chem. Eng. J. 352 (2018) 664–672.

S5 M. Pan, H. Zhang, G. Gao, L. Liu, W. Chen, Facet-dependent catalytic activity of nanosheet-assembled bismuth oxyiodide microspheres in degradation of bisphenol A, Environ. Sci. Technol. 49 (2015) 6240–6248.

S6 X. Shi, P. Wang, L. Wang, Y. Bai, H. Xie, Y. Zhou, J. A. Wang, Z. Li, L. Qu, M. Shi, L. Ye, Few layered BiOBr with expanded interlayer spacing and oxygen vacancies for efficient decomposition of real oil field produced wastewater, ACS Sustainable Chem. Eng. 6 (2018) 13739–13746.